

## The electronic contribution to the thermal conductivity of layered high- $T_c$ materials

This article has been downloaded from IOPscience. Please scroll down to see the full text article.

1996 J. Phys.: Condens. Matter 8 2043

(<http://iopscience.iop.org/0953-8984/8/12/016>)

View [the table of contents for this issue](#), or go to the [journal homepage](#) for more

Download details:

IP Address: 171.66.16.208

The article was downloaded on 13/05/2010 at 16:26

Please note that [terms and conditions apply](#).

## The electronic contribution to the thermal conductivity of layered high- $T_c$ materials

M Houssa†, M Ausloos‡ and S Sergeenkov§

SUPRAS Institut de Physique B5, Université de Liège, B-4000 Liège, Belgium

Received 14 November 1995

**Abstract.** We have used the variational approach to calculate the in-plane electronic thermal conductivity of high- $T_c$  superconductors along the lines of a two-fluid model. To account for the layered structure of these compounds, an anisotropic electronic energy spectrum with a Josephson-like coupling between the superconducting planes within a Lawrence–Doniach model has been assumed. Both elastic and inelastic electronic scattering processes are considered. The theoretical results obtained are in *quantitative agreement* with experimental data on  $\text{Bi}_2\text{Sr}_2\text{CaCu}_2\text{O}_8$  single crystals and  $\text{Bi}_2\text{Sr}_2\text{Ca}_2\text{Cu}_3\text{O}_{10}$  polycrystals. These results suggest an electronic origin of the peak observed in the thermal conductivity of these materials.

### 1. Introduction

The thermal conductivity  $\kappa$  still remains a controversial transport property of high-critical-temperature superconductors (HTSs). Some authors attribute the main structure of this transport coefficient, the rapid increase of  $\kappa$  below  $T_c$  and the peak at lower temperature, to the lattice contribution  $\kappa_p$  of the thermal conductivity [1–3]. The rapid rise of  $\kappa$  in the superconducting state is then attributed to the increase of phonon mean free path as electrons condense into Cooper pairs which do not scatter phonons. Yu *et al* [4] have however proposed an alternative interpretation based on a two-fluid model for superconductivity: as the scattering rate of normal electrons has been observed to decrease rapidly in the superconducting state of  $\text{YBa}_2\text{Cu}_3\text{O}_{7-\delta}$  [5] and  $\text{Bi}_2\text{Sr}_2\text{CaCu}_2\text{O}_8$  [6], the rapid increase of  $\kappa$  below  $T_c$  could be mainly due to an electronic contribution. A phenomenological description of this contribution has been suggested [7] and has been applied to describe the behaviour of  $\kappa$  in  $\text{YBa}_2\text{Cu}_2\text{O}_{7-\delta}$  ceramics, pure or doped with Fe, and presenting or not an excess of CuO [8].

In the present paper, the electronic contribution to the thermal conductivity of HTSs is calculated using the variational method introduced by Kohler and described by Ziman [9]. This approach is quite powerful as it allows one to take into account the dimensionality and the anisotropy of compounds such as HTSs in a straightforward way. In this approach, the transport coefficients are tensors expressed in terms of trial currents and scattering matrix elements. We have calculated the in-plane thermal conductivity  $\kappa_{e,ab}$  of HTSs, taking into account the layered structure of these materials using an anisotropic electronic energy

† e-mail: houssa@gw.unipc.ulg.ac.be.

‡ e-mail: ausloos@gw.unipc.ulg.ac.be.

§ Present address: Department of Chemistry, Texas Christian University, POB 32908, Fort Worth, TX 76129, USA.

spectrum, with a Josephson-like coupling between the superconducting planes (as in the Lawrence–Doniach model [10]). We have considered elastic and inelastic scattering of electrons by acoustic phonons as well as elastic scattering of electrons by impurities. We have not taken into account the scattering of electrons by grain boundaries, dislocations and sheetlike faults in order to limit the number of free parameters in the final expression for  $\kappa$ . We have also neglected the scattering of electrons by high-frequency optical phonons since they are not excited in the temperature region of interest, i.e. below 200 K.

In section 2, we present the general tensorial variational expression for the electronic thermal conductivity of an anisotropic system. The scattering processes of electrons are discussed in section 3. In section 4, we present and discuss the theoretical results. The model is tested on the experimental data of Allen *et al* [11] on a single crystal of  $\text{Bi}_2\text{Sr}_2\text{CaCu}_2\text{O}_8$  and on the data of Cloots *et al* [12] on a polycrystalline sample of  $\text{Bi}_2\text{Sr}_2\text{Ca}_2\text{Cu}_3\text{O}_{10}$ . Conclusions are finally drawn in section 5.

## 2. A variational expression for the in-plane electronic thermal conductivity

Layered high- $T_c$  compounds such as the bismuth and thallium families have a tetragonal lattice for which transport coefficients are diagonal tensors. The tensorial expression for the electronic thermal conductivity of such systems is given in the variational scheme by [9, 13]

$$\kappa_e^{\mu\mu} = \frac{1}{T} \left[ \sum_{ij} U_i^{\mu\mu} Q_{ij}^{\mu\mu} U_j^{\mu\mu} - \left( \sum_{ij} J_i^{\mu\mu} Q_{ij}^{\mu\mu} U_j^{\mu\mu} \right)^2 / \sum_{ij} J_i^{\mu\mu} Q_{ij}^{\mu\mu} J_j^{\mu\mu} \right] \quad (1)$$

where  $\mu = (x, y, z)$  and where  $J_i^{\mu\mu}$  and  $U_i^{\mu\mu}$  are the trial currents defined by

$$\begin{aligned} J_i^{\mu\mu} &= -e \int d\mathbf{k} \left( -\frac{\partial f^0}{\partial E} \right) v_\mu(\mathbf{k}) \phi_i^\mu(\mathbf{k}) \\ U_i^{\mu\mu} &= \int d\mathbf{k} \left( -\frac{\partial f^0}{\partial E} \right) E(\mathbf{k}) v_\mu(\mathbf{k}) \phi_i^\mu(\mathbf{k}) \end{aligned} \quad (2)$$

with  $-e$  the electron charge,  $v_\mu(\mathbf{k})$  the  $\mu$  component of the electron velocity with wave vector  $\mathbf{k}$ ,  $E(\mathbf{k}) = \sqrt{(\varepsilon(\mathbf{k}) - \varepsilon_F)^2 + \Delta^2(\mathbf{k})}$  the quasiparticle energy spectrum with  $\varepsilon_F$  the Fermi energy and  $\Delta$  the superconducting gap parameter,  $f^0$  the Fermi–Dirac distribution function and  $Q_{ij}^{\mu\mu} = (P^{-1})_{ij}^{\mu\mu}$ , with  $P_{ij}^{\mu\mu}$  the elements of the scattering matrix  $\mathbf{P}$  given by

$$P_{ij}^{\mu\mu} = \int d\mathbf{k}' \int d\mathbf{k} C(\mathbf{k}, \mathbf{k}') \left[ \phi_i^\mu(\mathbf{k}) - \phi_i^\mu(\mathbf{k}') \right] \left[ \phi_j^\mu(\mathbf{k}) - \phi_j^\mu(\mathbf{k}') \right] \quad (3)$$

where  $C(\mathbf{k}, \mathbf{k}')$  is the scattering probability corresponding to the different electronic scattering processes and  $\phi_i^\mu(\mathbf{k})$  the trial functions.

We have considered a BCS s-wave pairing with a temperature dependence of the gap approximately by [4, 14]

$$\Delta(T) = \Delta(0) \tanh(\alpha \sqrt{(T_c - T)/T}) \quad (4)$$

where the constant  $\alpha \approx 2$ .

In order to take into account the layered structure of HTSs, we have considered an anisotropic electronic energy spectrum with a Josephson coupling energy  $J_c$  between the superconducting ( $\text{CuO}_2$ ) planes [10]

$$\varepsilon(\mathbf{k}) = \frac{\hbar^2}{2m_{ab}^*} (k_x^2 + k_y^2) + J_c \cos(k_z d) \quad (5)$$

where  $m_{ab}^*$  is the effective mass of electron in the  $ab$  plane and  $d$  the distance between the superconducting planes. The coupling energy  $J_c$  is given by [10]

$$J_c = \sqrt{4\varepsilon_F \hbar^2 / m_c^* d^2} \quad (6)$$

with  $m_c^*$  the effective mass of electrons along the  $c$  axis.

We have then performed calculations of the in-plane electronic thermal conductivity  $\kappa_{e,ab}$ , i.e. supposing that the temperature gradient lies along the  $ab$  planes as is most usually the case. To this end, we have used the set of trial functions  $\phi_i^\mu(\mathbf{k}) = E(\mathbf{k})^{i-1} k_\mu$  limited to  $i = 1, 2$  [9, 15]. As a result, the in-plane trial currents defined in (2) read, in the long-wavelength limit ( $k_z d \ll 1$ , so that  $\cos(k_z d) \approx 1$ ),

$$\begin{aligned} J_1^{ab} &= J_0^{ab} (k_B T) K_0(T) \\ J_2^{ab} &= J_0^{ab} (k_B T)^2 K_1(T) \\ U_1^{ab} &= U_0^{ab} (k_B T)^2 K_1(T) \\ U_2^{ab} &= U_0^{ab} (k_B T)^3 K_2(T) \end{aligned} \quad (7)$$

where  $J_0^{ab} = (-e)2\pi^2 m_{ab}^* / d \hbar^3$  and  $U_0^{ab} = J_0^{ab} / (-e)$ , and

$$K_n(T) = \int_{b(T)}^{\infty} \frac{x^n (x - j_c)}{\cosh^2(x/2)} dx \quad (8)$$

with  $x = E/k_B T$ ,  $j_c = J_c/k_B T$ , and  $b(T) = \sqrt{\Delta^2 + J_c^2}/k_B T$ .

### 3. Electronic scattering mechanisms

The scattering processes restore the equilibrium state of a system which has been submitted to an external perturbation such as an electric field or a temperature gradient. We consider here the elastic scattering of electrons by impurities and the inelastic scattering of electrons by acoustical phonons.

#### 3.1. Electron–impurity scattering

HTSs are non-stoichiometric systems which contain point defects mainly corresponding to oxygen atom vacancies. In order to take into account the scattering of electrons by these ‘impurities’, we have used the Yukawa potential [9]

$$V(r) = (Ze^2/\varepsilon_c) e^{-\Gamma^{2D} r} / r \quad (9)$$

where  $Ze$  is the effective charge of the impurity,  $\varepsilon_c$  the effective dielectric constant and  $\Gamma^{2D}$  the two dimensional Thomas–Fermi factor which takes into account the screening of the electronic density near the impurity [16]

$$\Gamma^{2D} = 2m_{ab}^* e^2 / 4\pi \hbar^2 \varepsilon_0 \quad (10)$$

where  $\varepsilon_0$  is the electric permittivity in vacuum.

In the Born approximation, the (elastic) electron–impurity scattering probability corresponding to the Yukawa potential (9) is given by

$$\begin{aligned} C^{(imp)}(\mathbf{k}, \mathbf{k}') &= (16\pi^3/\hbar)(Ze^2/V\varepsilon_c)^2 \left[ N / \left( |\mathbf{k} - \mathbf{k}'|^2 \right. \right. \\ &\quad \left. \left. + (\Gamma^{2D})^2 \right)^2 \right] f^0(E) [1 - f^0(E')] \delta(E - E') \end{aligned} \quad (11)$$

where  $V$  is the volume of the crystal,  $N$  the impurity fraction in the sample, and  $\mathbf{k}$  and  $\mathbf{k}'$  the wave vectors of the incoming and outgoing electron respectively. Inserting (11) in (3) and integrating in cylindrical coordinates, we obtain the following expressions for the in-plane scattering matrix elements for electron–impurity collisions in the long-wavelength limit:

$$P_{ij,ab}^{el-imp} = P_{0,ab}^{imp} (k_B T)^{i+j-5/2} I_{i+j-2}^{ab}(T) \quad (12)$$

where

$$P_{0,ab}^{imp} = 16(\pi^7 n / \hbar^4 V) [(2m_{ab}^*)^{3/2} / \Gamma^{2D} d^2] (Ze^2 / \epsilon_c)^2 N \quad (13)$$

is a material constant, and

$$I_k^{ab}(T) = \int_{b(T)}^{\infty} \frac{x^k (x - j_c)}{(1 + \cosh(x))(4(x - j_c) + y)^{3/2}} dx \quad (14)$$

with  $y = (k_B T)^{-1} [\hbar^2 (\Gamma^{2D})^2 / 2m_{ab}^*]$ .

### 3.2. Electron–acoustic phonon scattering

The scattering of electrons with acoustic phonons is described using the deformation potential approximation [9, 13]

$$V(q) = -i\sqrt{\hbar/2M\omega_q} \lambda_{ab} \epsilon_F q \quad (15)$$

where  $q$  is the phonon wave vector,  $\lambda_{ab}$  the in-plane electron–phonon coupling constant,  $\omega_q$  the phonon frequency,  $M$  the mass of the crystal, and  $\epsilon_F$  the Fermi energy. Note that this approximation is valid in the case of long-wavelength acoustic phonons which are supposed to limit predominantly heat transport in high- $T_c$  cuprates [1, 3]. We have assumed a linear in-plane acoustic phonon spectrum  $\hbar\omega_q = \hbar s q$ , with  $s$  the sound velocity in the crystal.

In the Born approximation, the scattering probability corresponding to the potential (15) reads

$$C^{(ph)}(\mathbf{k}, \mathbf{k}') = (V/8\pi^2) [(\lambda_{ab} \epsilon_F q)^2 / M\omega_q] f^0(E) [1 - f^0(E')] N_q \delta(E - E' + \hbar\omega_q) \quad (16)$$

where  $V$  is the volume of the crystal and  $N_q$  the Bose–Einstein distribution function. We suppose here that the phonon system is in equilibrium, i.e. we neglect the phonon drag contribution.

Inserting expression (16) into (3) and integrating in cylindrical coordinates, we obtain the in-plane electron–acoustic phonon scattering matrix elements

$$\begin{aligned} P_{11,ab}^{el-ac.ph} &= P_{0,ab}^{ac.ph} (k_B T)^3 G_{30}^{ab}(T) \\ P_{12,ab}^{el-ac.ph} &= P_{0,ab}^{ac.ph} (k_B T)^4 \left\{ G_{31}^{ab}(T) + G_{40}^{ab}(T) \right\} \\ P_{22,ab}^{el-ac.ph} &= P_{0,ab}^{ac.ph} (k_B T)^5 \left\{ G_{32}^{ab}(T) + 2G_{41}^{ab}(T) + G_{50}^{ab}(T) + t^{-1} \left( G_{31}^{ab}(T) - j_c G_{30}^{ab}(T) \right) \right\} \end{aligned} \quad (17)$$

where

$$P_{0,ab}^{ac.ph} = (2\pi/\hbar^6) (V/Ms^4) [(\lambda_{ab} \epsilon_F)^2 / d^2] (m_{ab}^*)^2 \quad (18)$$

and

$$G_{km}^{ab}(T) = \int_{b(T)}^{\infty} \frac{x^m}{(e^x + 1)} \int_0^{u_{\max}} du \frac{u^k ((4(x - j_c)/t) - u^2)^{-1/2}}{(e^u - 1)(e^{-(x+u)} + 1)} \quad (19)$$

with  $t = k_B T / 2m_{ab}^* s^2$ ,  $u = \hbar\omega / k_B T$  and

$$u_{\max} = \begin{cases} 2\sqrt{(x - j_c)/t} & \text{if } 2\sqrt{(x - j_c)/t} \leq T_D/T \\ T_D/T & \text{if } 2\sqrt{(x - j_c)/t} > T_D/T \end{cases}$$

assuming thus the usual Debye cut-off procedure for the phonon spectrum ( $T_D$  is the Debye temperature).

Note that an attempt to go beyond this approximation has been discussed in [17].

### 3.3. Total electronic scattering

According to Matthiessen's rule [9], which is expected to hold in HTSs, the total scattering rate of electrons is the sum of the individual electronic scattering rates

$$P_{ij}^{el,tot} = P_{ij}^{el,imp} + P_{ij}^{el,ac.ph}. \quad (20)$$

Consequently, the total in-plane electronic thermal conductivity  $\kappa_{e,ab}$  is obtained by summing the electronic scattering probabilities (12) and (17), and inserting these latter expressions with the trial currents (7) in to the general expression (1).

## 4. Results and discussion

The normalized superconducting state in-plane electronic thermal conductivity  $\kappa_{e,ab}(T) / \kappa_{e,ab}(T_c)$  due to electron-impurity and electron-phonon scattering is shown in figure 1. Let us observe that  $\kappa_{e,ab}$  decreases rapidly below  $T_c$  when only impurity scattering is considered whereas  $\kappa_{e,ab}$  increases below  $T_c$  and reaches a maximum at about  $0.6T_c$  when inelastic electron-phonon collisions are taken into account; this latter contribution then falls off at lower temperatures because of the condensation of charge carriers into Cooper pairs.

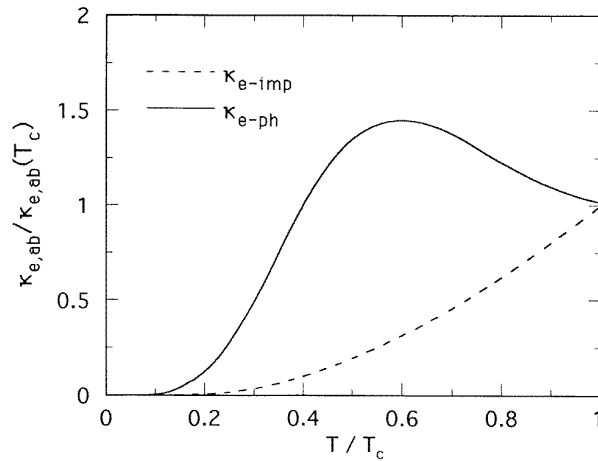


**Figure 1.** The temperature dependence of the normalized superconducting state in-plane electronic thermal conductivity  $\kappa_{e,ab}(T) / \kappa_{e,ab}(T_c)$  for electron-impurity (---) and electron-phonon (—) scattering. The coupling energy  $J_c$  has been fixed to  $10^{-3}$  eV.

The total normalized in-plane electronic thermal conductivity, including electron-phonon and electron-impurity scattering is illustrated in figure 2. We have fixed the value of

$\lambda_{ab}$  to 0.5 [18] and  $J_c$  to  $10^{-3}$  eV and calculated  $\kappa_{e,ab}$  for several impurity fractions  $N$  in the system. One can see that  $\kappa_{e,ab}$  is quasi-constant in the normal state and independent of  $N$ , suggesting that the normal state electronic thermal conductivity is mainly due to electron-phonon scattering. In the superconducting state, the maximum value of  $\kappa_{e,ab}$  decreases and is shifted towards higher temperature as the impurity fraction  $N$  is increased, similarly to the situation for an isotropic model [19].

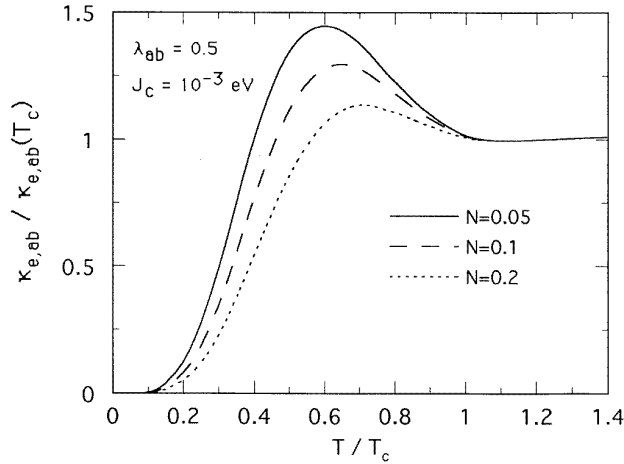


**Figure 2.** The total normalized in-plane electronic thermal conductivity  $\kappa_{e,ab}(T)/\kappa_{e,ab}(T_c)$  against reduced temperature  $T/T_c$  for several impurity fractions  $N$  in the system. The electron-phonon coupling constant  $\lambda_{ab}$  and the inter-layer coupling energy  $J_c$  have been fixed respectively to 0.5 and  $10^{-3}$  eV.

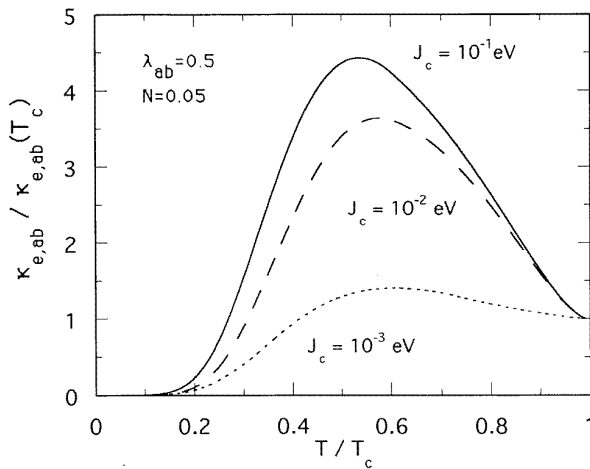


**Figure 3.** Normalized in-plane electronic thermal conductivity  $\kappa_{e,ab}(T)/\kappa_{e,ab}(T_c)$  as a function of the reduced temperature  $T/T_c$  for a fixed value of the electron-phonon coupling constant  $\lambda = 0.5$ , the impurity fraction  $N = 0.05$  and several values of the inter-layer coupling energy  $J_c$ .

The influence of the interlayer coupling constant  $J_c$  on the temperature dependence of the

electronic thermal conductivity is shown in figure 3 for a fixed value of the electron–phonon coupling constant  $\lambda_{ab} = 0.5$  and the impurity fraction  $N = 0.05$ . The amplitude of the maximum is decreased and its position is shifted towards higher temperatures as the coupling energy is decreased, i.e. when the system becomes more two dimensional. This behaviour can be interpreted as follows. As  $J_c$  is decreased, the area of the cylindrical Fermi surface is lowered, which results in a decrease of heat carrying electrons. Moreover, the mean free path of electrons decreases when  $J_c$  decreases since electrons are then more ‘constrained’ to move in the  $\text{CuO}_2$  planes where they are more strongly scattered by impurities and phonons. As a result, the maximum of  $\kappa_{e,ab}$  is less pronounced when  $J_c$  is decreased.

Consequently, the different behaviour of the thermal conductivity in  $\text{YBa}_2\text{Cu}_3\text{O}_{7-\delta}$  and  $\text{Bi}_2\text{Sr}_2\text{CaCu}_2\text{O}_8$ , namely the less pronounced maximum observed in the latter compounds [3, 4, 11], could be due to a more layered and anisotropic structure of  $\text{Bi}_2\text{Sr}_2\text{CaCu}_2\text{O}_8$ .

Experimental data on the thermal conductivity of  $\text{Bi}_2\text{Sr}_2\text{CaCu}_2\text{O}_8$  have been reported in several publications so far [11, 20–22]. We have chosen to fit the results of Allen *et al* [11] as they allowed us to separate the electron and phonon contribution in a subtle way (see below). In order to reproduce these data, we have fixed the following values of the physical parameters [23–26]:  $T_c = 85$  K,  $\varepsilon_F = 0.1$  eV,  $\Delta(0) = 20$  meV,  $\varepsilon_c = 35$ ,  $\Gamma^{2D} = 30.3 \text{ \AA}^{-1}$ ,  $m_{ab}^* = 8m_0$ , where  $m_0$  is the free electron mass,  $\gamma = \sqrt{m_c^*/m_{ab}^*} \approx 50$ ,  $d = 3 \text{ \AA}$ ,  $T_D = 250$  K and  $s = 3500 \text{ m s}^{-1}$ . The corresponding value of the coupling energy  $J_c$  calculated from (6) is  $4.7 \times 10^{-3}$  eV.

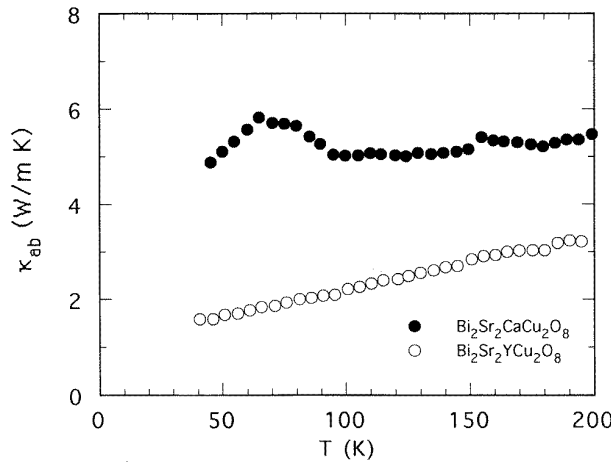


**Figure 4.** The temperature dependence of the in-plane thermal conductivity of a superconducting single crystal of  $\text{Bi}_2\text{Sr}_2\text{CaCu}_2\text{O}_8$  (●) and an insulating single crystal of  $\text{Bi}_2\text{Sr}_2\text{YCu}_2\text{O}_8$  (○) as derived from [11].

The experimental results of Allen *et al* [11] on the in-plane thermal conductivity of a superconducting single crystal of  $\text{Bi}_2\text{Sr}_2\text{CaCu}_2\text{O}_8$  (●) and an insulating crystal of  $\text{Bi}_2\text{Sr}_2\text{YCu}_2\text{O}_8$  (○) are shown in figure 4. Since the phonon spectra of these two materials are almost the same [27], one can reasonably assume that the phonon contribution  $\kappa_{ph}$  of the superconducting sample is nearly identical to the insulating one which monotonically increases with temperature (see figure 4). Consequently, the electronic contribution  $\kappa_{e,ab}$  of the single crystal of  $\text{Bi}_2\text{Sr}_2\text{CaCu}_2\text{O}_8$  is obtained from the total contribution by subtracting the phonon background which corresponds to the thermal conductivity of  $\text{Bi}_2\text{Sr}_2\text{YCu}_2\text{O}_8$  [11].



The best fit to the electronic thermal conductivity of the single crystal of  $\text{Bi}_2\text{Sr}_2\text{CaCu}_2\text{O}_8$  so obtained is shown in figure 5. The data are quite well reproduced over the entire range of temperatures with realistic values of the free parameters:  $\lambda_{ab} = 0.42$ ,  $N = 0.06$  and  $J_c = 2 \times 10^{-3}$  eV.

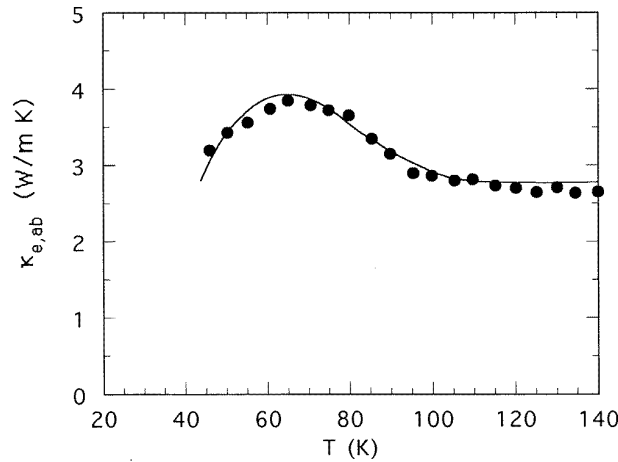


**Figure 5.** The in-plane electronic thermal conductivity of a single crystal of  $\text{Bi}_2\text{Sr}_2\text{CaCu}_2\text{O}_8$  [11] against temperature (●) and the calculated theoretical fit (—) along the variational method. See the text for the values of the free parameters.

We have used the data of Cloots *et al* [12] for examining a 2223 compound. It should be noted that the sample was obtained through a vitreous route which leads to a quite homogeneous sample. The thermal conductivity  $\kappa$  of this superconducting polycrystal of  $\text{Bi}_2\text{Sr}_2\text{Ca}_2\text{Cu}_3\text{O}_{10}$  is shown in figure 6. The critical temperature, estimated via electrical resistivity measurements, is about 110 K [12]. The behaviour of the thermal conductivity, measured using a steady state and longitudinal heat flow method described in [8], is in agreement with previous data on polycrystalline systems [18, 28–30]:  $\kappa$  monotonically decreases with decreasing temperature in the normal state, a slope break occurs at  $T_c$  and  $\kappa$  reaches a maximum at about 85 K;  $\kappa$  then falls off at lower temperatures.

Since the substitution of Ca in  $\text{Bi}_2\text{Sr}_2\text{Ca}_2\text{Cu}_3\text{O}_{10}$  by rare earth or yttrium atoms has not yet been successfully achieved, we have to use another method to separate the electronic and phonon contribution of the thermal conductivity. First, as in [8], we suppose that  $\kappa$  can be separated into an intergrain contribution  $\kappa_{gb}$  from grain boundaries and an intragrain  $\kappa_{ig}$  contribution due to the flow of electrons and phonons, i.e.  $\kappa = \kappa_{ig} + \kappa_{gb}$ .

The intergrain contribution is estimated by using a percolation model [31]. We found that  $\kappa_{gb} \approx 0.4\kappa$ , leading to  $\kappa_{ig} \approx 0.6\kappa$ . The electronic contribution is then obtained by subtracting a phonon background from  $\kappa_{ig}$ . This background is obtained by fitting normal state data which monotonically increase with temperature (figure 6) and taking into account the value of the normal state electronic thermal conductivity  $\kappa_e^n \approx 0.15 \text{ W mK}^{-1}$  estimated via the Wiedemann–Franz law. The temperature dependence of the electronic contribution to the thermal conductivity of the  $\text{Bi}_2\text{Sr}_2\text{Ca}_2\text{Cu}_3\text{O}_{10}$  polycrystal so derived is shown in figure 7 with the theoretical curve obtained by using the following physical parameters [23–26, 32]:  $T_c = 110 \text{ K}$ ,  $\varepsilon_F = 0.1 \text{ eV}$ ,  $\Delta(0) = 20 \text{ meV}$ ,  $\varepsilon_c = 35$ ,  $\Gamma^{2D} = 15.15 \text{ \AA}^{-1}$ ,  $m_{ab}^* = 4m_0$ ,  $\gamma \approx 30$ ,  $d = 6.7 \text{ \AA}$ ,  $T_D = 275 \text{ K}$  and  $s = 3500 \text{ m s}^{-1}$ . The corresponding value of the coupling energy  $J_c$  calculated from (6) is  $3.9 \times 10^{-3} \text{ eV}$ . The values of the

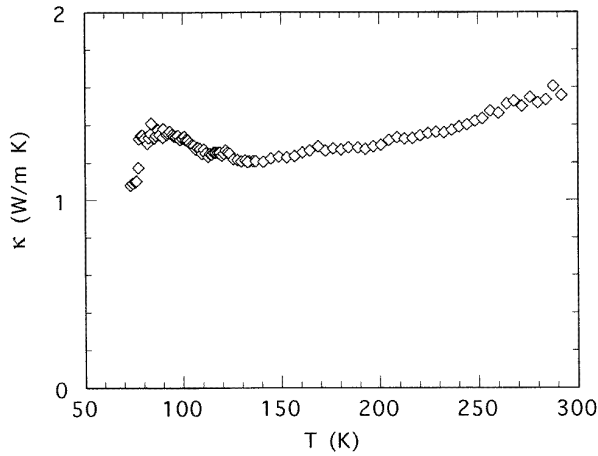


**Figure 6.** The temperature dependence of the thermal conductivity of a polycrystalline sample of  $\text{Bi}_2\text{Sr}_2\text{Ca}_2\text{Cu}_3\text{O}_{10}$  [12].

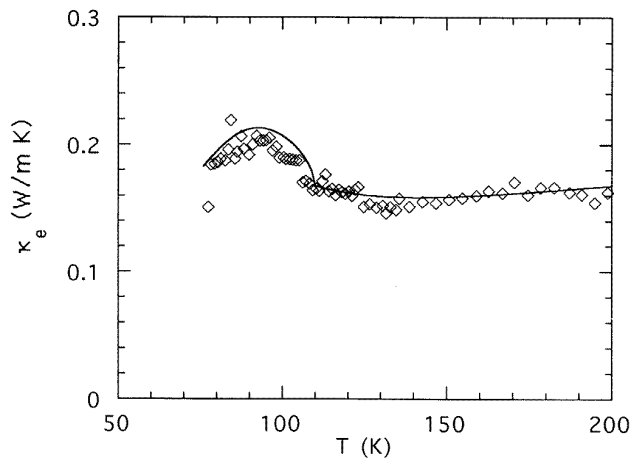


**Figure 7.** The electronic thermal conductivity of the polycrystalline sample of  $\text{Bi}_2\text{Sr}_2\text{Ca}_2\text{Cu}_3\text{O}_{10}$  [12] ( $\diamond$ ) and the best fit (—) along the variational method. See the test for the values of the free parameters.

free parameters obtained from the fit are  $\lambda_{ab} = 0.58$ ,  $N = 0.41$  and  $J_c = 3 \times 10^{-3}$  eV. As in the case of Bi-2212, the data are quite well reproduced with realistic values of the free parameters. Notice that the impurity fraction is rather high (40%), which seems reasonable as the sample of Bi-2223 is a (granular) polycrystal containing some 2212 phases.

## 5. Conclusions

In light of the possible electronic origin of the thermal conductivity peak of HTSs, we have derived the electronic contribution to the thermal conductivity of highly anisotropic layered materials using a variational method along the lines of a two-fluid model. We have considered an anisotropic electronic energy spectrum with an interlayer coupling energy

between the superconducting planes. Taking into account elastic and inelastic electron scattering by impurities and acoustic phonons, we have obtained theoretical results which reproduce reasonably well the experimental data of Allen *et al* [11] on a single crystal of  $\text{Bi}_2\text{Sr}_2\text{CaCu}_2\text{O}_8$  and the data of Cloots *et al* [12] on a polycrystal of  $\text{Bi}_2\text{Sr}_2\text{Ca}_2\text{Cu}_3\text{O}_{10}$  with quite realistic values of the free parameters.

### Acknowledgments

Part of this work has been financially supported through the Impulse Program on High-Temperature Superconductors of Belgium Federal Services for Scientific, Technological and Cultural (SSTC) Affairs under contract SU/02/013 and through the ARC (94-99/174) grant from the Minister of High Education and Research to the University of Liege. We are grateful to Dr K Durczewski for his comments and interest. We thank Dr R Cloots and Dr H Bougrine for providing us with the data on the  $\text{Bi}_2\text{Sr}_2\text{Ca}_2\text{Cu}_3\text{O}_{10}$  polycrystal.

### References

- [1] Tewordt L and Wölkhausen Th 1989 *Solid State Commun.* **70** 839
- [2] Uher C 1990 *J. Supercond.* **3** 337
- [3] Peacor S D, Richardson R A, Nori F and Uher C 1991 *Phys. Rev. B* **44** 9508
- [4] Yu R C, Salamon M B, Lu J P and Lee W C 1992 *Phys. Rev. Lett.* **69** 1431
- [5] Bonn D A, Dosanjh P, Liang R and Hardy W N 1992 *Phys. Rev. Lett.* **68** 2390
- [6] Romero D B, Porter C D, Tanner D B, Forro L, Mandrus D, Mihaly L, Carr G L and Williams G P 1992 *Phys. Rev. Lett.* **68** 1590
- [7] Ausloos M and Houssa M 1993 *Physica C* **218** 15
- [8] Houssa M, Bougrine H, Ausloos M, Grandjean I and Mehbood M 1994 *J. Phys.: Condens. Matter* **6** 6305
- [9] Kohler M 1948 *Z. Phys.* **124** 772; 1949 *Z. Phys.* **126** 495  
Ziman J H 1963 *Electrons and Phonons* (Oxford: Clarendon)
- [10] Lawrence W and Doniach S 1971 *Proc. 12th Int. Conf. on Low Temperature Physics (Kyoto 1971)* ed E Kanda (Academic Press of Japan, Tokyo) p 361
- [11] Allen P B, Du X, Mihaly L and Forro L 1994 *Phys. Rev. B* **49** 9073
- [12] Cloots R, Bougrine H, Houssa M, Stassen S, D'Urzo L, Rulmont A and Ausloos M 1994 *Physica C* **231** 259
- [13] Durczewski K and Ausloos M 1985 *J. Magn. Magn. Mater.* **53** 243
- [14] Xu J H, Shen J L, Miller J L Jr and Ting C S 1994 *Phys. Rev. Lett.* **73** 2492
- [15] Bardeen J, Rickayzen G and Tewordt L 1959 *Phys. Rev.* **113** 982
- [16] Giuliani G F and Quinn J J 1982 *Phys. Rev. B* **26** 4421
- [17] Durczewski K and Ausloos M 1994 *Z. Phys. B* **94** 57
- [18] Dey T K, Barik H K and Chopra K L 1991 *Solid State Commun.* **80** 185
- [19] Houssa M and Ausloos M 1994 *Physica C* **235–20** 1483
- [20] Crommie M F and Zettl A 1990 *Phys. Rev. B* **41** 10978
- [21] Crommie M F and Zettl A 1991 *Phys. Rev. B* **43** 408
- [22] Du X, Mihaly L and Allen P B 1994 *Physica B* **194–196** 1507
- [23] Harshman D R and Mills A P 1992 *Phys. Rev. B* **45** 10684
- [24] Koltun R, Hoffmann M, Splittgerber-Hünnekes P C and Güntherodt G 1990 *Physica B* **165–166** 1567
- [25] Farrel D E, Bonham S, Foster J, Change Y C, Jiang P Z, Vandervoort K G, Lam D J and Kogan V G 1989 *Phys. Rev. Lett.* **63** 782
- [26] Baumgart P, Blumenröder S, Erle A, Hillebrands B, Splittgerber P, Güntherodt G and Schmidt H 1989 *Physica C* **162–164** 1073
- [27] Renker B, Gompf F, Ewert D, Adelman P, Schmidt H, Gering E and Mukta H 1989 *Z. Phys. B* **77** 65
- [28] Jezowski A 1990 *Solid State Commun.* **75** 779
- [29] Dey T K and Barik H K 1992 *Solid State Commun.* **82** 673
- [30] Bhattacharya D and Maiti H S 1993 *Physica C* **216** 147
- [31] Kirichenko Y A, Kozlov S M, Rusanov K V, Tyurina E G, Titova S G and Fotiev V A 1991 *Superconductivity* **4** 2256
- [32] Matsubara I, Tanigawa H, Ogura T, Yamashita H and Kinoshita M 1992 *Phys. Rev. B* **45** 7414